

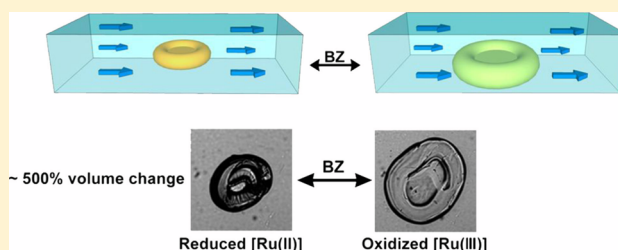
# Giant Volume Change of Active Gels under Continuous Flow

Ye Zhang,<sup>†,§</sup> Ning Zhou,<sup>†,§</sup> Ning Li,<sup>‡</sup> Megan Sun,<sup>†</sup> Dongshin Kim,<sup>‡</sup> Seth Fraden,<sup>\*,‡</sup> Irving R. Epstein,<sup>\*,†</sup> and Bing Xu<sup>\*,†</sup>

<sup>†</sup>Department of Chemistry and <sup>‡</sup>Department of Physics, Brandeis University, 415 South Street, Waltham, Massachusetts 02454, United States

**S** Supporting Information

**ABSTRACT:** While living systems have developed highly efficient ways to convert chemical energy (e.g., ATP hydrolysis) to mechanical motion (e.g., movement of muscle), it remains a challenge to build muscle-like biomimetic systems to generate mechanical force directly from chemical reactions. Here we show that a continuous flow of reactant solution leads to by far the largest volume change to date in autonomous active gels driven by the Belousov–Zhabotinsky reaction. These results demonstrate that microfluidics offers a useful and facile experimental approach to optimize the conditions (e.g., fabrication methods, counterions, flow rates, concentrations of reagents) for chemomechanical transduction in active materials. This work thus provides much needed insights and methods for the development of chemomechanically active systems based on combining soft materials and microfluidic systems.



## INTRODUCTION

This paper reports the use of a continuous reactant flow in a microfluidic system to achieve giant oscillating volume changes in spontaneously active gels for chemomechanical transduction. Conversion of the energy stored in chemical bonds into mechanical forces is an essential process for life. Living systems have evolved thermodynamically efficient and environmentally benign ways of harnessing chemical energy to produce motion, for example, using the energy released by ATP hydrolysis to power the directed movement of muscle fibers or microtubules.<sup>1</sup> On the other hand, current man-made systems (e.g., internal combustion engines), though able to convert chemical energy into mechanical forces or movement,<sup>2</sup> have much lower efficiency than biological systems. Thus, it is attractive to construct biomimetic systems that preserve the key aspects of living systems for generating mechanical forces from chemical reactions. Inspired by a prominent feature of muscle, softness, researchers have extensively explored gels as a type of synthetic material for mimicking muscle.<sup>3–7</sup> Among the active soft materials, one notable example is the spontaneous oscillating gels driven by the Belousov–Zhabotinsky (BZ) reaction<sup>8</sup> reported first by Yoshida.<sup>4</sup> Although it successfully integrates chemical oscillation with soft materials to give beating that resembles the behavior of heart muscle cells, the Yoshida gel exhibits relatively small volume change (~17%) during each cycle. Subsequent structural modification of the polymeric networks in gels of this type has resulted in only modest improvement.<sup>6,7,9</sup> These results imply that, in addition to softness, it is necessary to mimic other features of muscle in order to optimize chemomechanical transduction.

In research on biomimetic gel materials, an often overlooked anatomical feature is that capillaries play an integral role in vivo by providing biological fuels to and removing metabolic waste

from muscle cells. Thus, to explore gel materials in a muscle-like environment, we choose microfluidics<sup>10</sup> to simulate the effect of the capillary for chemical transportation. Several groups have explored gels in microfluidic systems.<sup>11–14</sup> For example, Beebe reported the use of gels as a component for self-regulated flow control<sup>9</sup> and adaptive liquid microlenses,<sup>5</sup> Kumacheva<sup>14</sup> and Seiffert<sup>12</sup> used microfluidic systems to generate capsules of biopolymer hydrogels, Herr demonstrated the use of gels for automated microfluidic protein blotting,<sup>13</sup> Wu utilized hydrogels to create complex, static solution gradients in microfluidic channels,<sup>15</sup> and Ismagilov employed nonlinear dynamic reactions in microfluidics to build a minimal functional model of hemostasis.<sup>16</sup> Although microfluidic systems have found application in studying the chemical communication<sup>17</sup> of BZ droplets and chemical self-organization,<sup>18</sup> the properties and potential of self-oscillating gels in a microfluidic system have yet to be explored for chemomechanical transduction.

In this work, we use a microfluidic channel (Scheme 1) to explore chemomechanical transduction in BZ catalyst-containing microgels made by photopolymerization (Figure 1). We observe that the volume change during each oscillation under optimal, continuous flow exceeds 500%, more than an order of magnitude greater than the highest reported value (25%)<sup>19</sup> for volume changes of oscillating gels without flow. Using a microfluidic system to study gels containing two new BZ catalysts (1 and 3, Figure 2B), we confirm that continuous flow generally results in larger volume changes than without flow. Besides easily tuning the flow rate, continuous flow allows us to switch the counterion of the BZ catalyst, thus revealing that the

Received: January 15, 2014

Published: April 21, 2014

## Scheme 1. Chemomechanical Oscillation of Active Gels with and without Flow of Solution

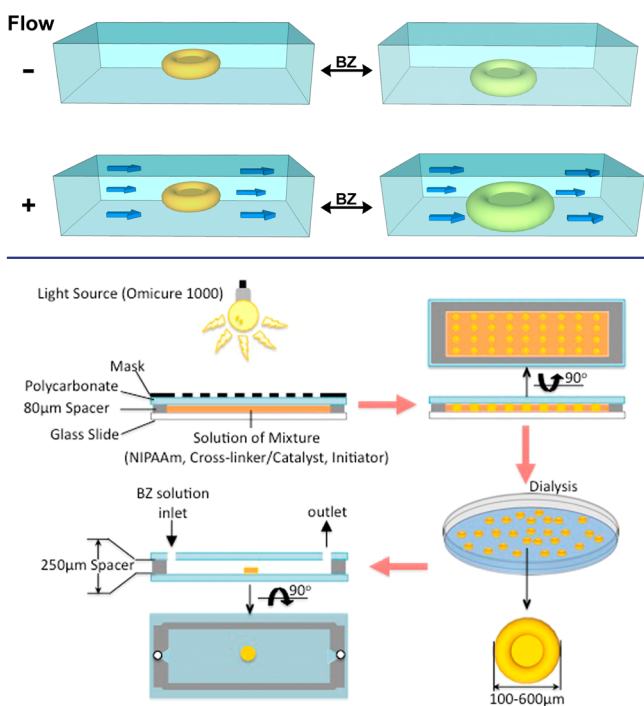


**Figure 1.** Setup for fabricating the microgel and the microfluidic channel for examining the volume change of the microgel.

nature and the charge of the electrolyte significantly affect the volume change of the oscillating gel. This work thus provides new insights and methods for the development of chemomechanical systems based on nonlinear chemical dynamics to impart specific multiple functionalities to novel soft materials.

## RESULTS AND DISCUSSION

Figure 1 shows the photopolymerization process for fabricating microgels. We employ rapid prototyping<sup>20</sup> to generate the photomasks, which are intended to create disk-shaped microgels with diameters of 100–600  $\mu\text{m}$ . We place the solutions containing the catalyst (1, 2, or 3), the monomer (4), and, if necessary, the cross-linker (5) (Figure 2A) into a polycarbonate mold (Figures 1 and S1, Supporting Information) with a height of 80  $\mu\text{m}$  to help define the height of the gel. After carrying out the photoinitiated polymerization<sup>9</sup> in an ice–water bath for 10–30 min, we obtain donut-shaped microgels, resulting from the reaction and diffusion of the reagents.<sup>21</sup> A subsequent 3-day dialysis in deionized (DI) water ensures the removal of any unreacted reagents from the microgel.

Using the procedure in Figure 1, we obtain three microgels,  $\text{Gel}_a$ ,  $\text{Gel}_b$ , and  $\text{Gel}_c$  (Figure 2B). In the three gels, the monomer, *N*-isopropylacrylamide (NIPAAm) (4), polymerizes to form poly(NIPAAm)<sup>22</sup> as the polymer backbone. In  $\text{Gel}_a$  and  $\text{Gel}_b$ , bis(*N,N'*-methylene-bis-acrylamide) (5), which serves as the cross-linker, and the BZ catalysts 1<sup>23</sup> and 2<sup>4</sup> as pendants copolymerize into the poly(NIPAAm) to form polymer network type I (Figure 2C). Catalyst 3,<sup>7</sup> which bears multiple polymerizable vinyl groups, itself acts as a cross-linker, so that  $\text{Gel}_c$  only requires the monomer 4 and the catalyst 3. Thus, the architecture of the polymer network in  $\text{Gel}_c$  differs from those in  $\text{Gel}_a$  and  $\text{Gel}_b$ , and we term it type II in this work.

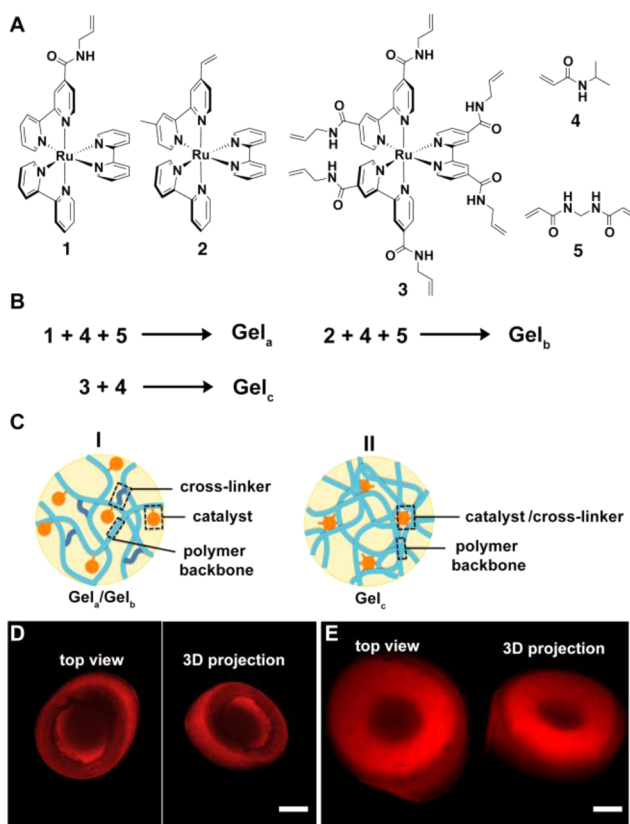


**Figure 2.** (A) Molecular structures of the components used for fabricating the oscillating gels. (B) Compositions of the three oscillating gels. (C) Schematic representations of the polymeric networks in the two types of gels. (D) Fluorescent images of a type I microgel ( $\text{Gel}_a$ ) viewed from its top and a 3D projection obtained from a z-scan (scale bar is 100  $\mu\text{m}$ ). (E) Fluorescent images of a type II microgel ( $\text{Gel}_c$ ) viewed from its top and a 3D projection obtained from a z-scan (scale bar is 100  $\mu\text{m}$ ).

For type I gels, the polymerization rate of NIPAAm (4) is 14% and 23% within  $\text{Gel}_a$  and  $\text{Gel}_b$ , respectively. The molar ratio of catalyst to NIPAAm is 0.5% and 0.6% in  $\text{Gel}_a$  and  $\text{Gel}_b$ , respectively. For the type II gel,  $\text{Gel}_c$ , the polymerization rate of NIPAAm is around 11%, and the molar ratio of catalyst (3) to NIPAAm is around 5%, almost 10 times as high as in the type I gels. These differences originate from the different structures of the catalysts and their different polymer networks in the gels.

Since the  $[\text{Ru}(\text{bipy})_3]^{2+}$ -based BZ catalysts (1,<sup>23</sup> 2,<sup>4</sup> and 3<sup>7</sup>) fluoresce upon irradiation at 488 nm, we use confocal fluorescent microscopy to characterize the shapes and structural properties of the microgels. As shown in typical examples (Figure 2D,E), both types of microgels show weaker fluorescence in their centers than at their edges. Together with the 3D projections, these results suggest that both types of microgels have donut-like shapes, that is, they are thicker at the edges than in the centers. This unique geometry may also contribute to the large volume change observed, in agreement with other works demonstrating geometry-enhanced volume changes.<sup>25</sup> Despite being fabricated under the same conditions, the microgels exhibit slight differences between batches. Additionally, inhomogeneity of the light source for polymerization results in a distribution of diameters and symmetries even within the same batch of microgels (Figure S2, Supporting Information).

The length of each dimension of the microgels is controlled to be below  $600\ \mu\text{m}$ , the critical length scale of the BZ wave, to guarantee the uniform oscillation of the microgels. To minimize the influence of size variation of the microgels on their oscillating volume change, microgels with the same size were picked for further tests.

Fluorescent images of thin slices of the microgels (Figure S3, Supporting Information) reveal different morphologies of the two types of gels. While the distribution of  $[\text{Ru}(\text{bipy})_3]^{2+}$  appears to be homogeneous in type I microgels ( $\text{Gel}_a$  and  $\text{Gel}_b$ ), type II microgels ( $\text{Gel}_c$ ) contain heterogeneously distributed  $[\text{Ru}(\text{bipy})_3]^{2+}$  centers, which agrees with our previous observation.

To test the chemomechanical oscillation behavior of the microgels in the presence of flow, we use a sandwich type of flow cell, constructed by gluing two pieces of polycarbonate film onto a  $250\ \mu\text{m}$  high spacer (Figure 1). A syringe pump connected to the inlet of the flow cell controls the flow rate of BZ solution through the cell. This simple setup (Figure S2, Supporting Information) fits under an optical microscope to allow an adapted CCD camera to record the oscillation of the microgel. The flow cell is placed on a temperature control stage (Figure S5, Supporting Information) to maintain constant temperature during the oscillation of the microgel. Using this microfluidic system, we first tested  $\text{Gel}_a$  under various BZ reaction conditions (Figure S6, Supporting Information) (e.g.,  $[\text{NaBrO}_3] = 0.08\text{--}0.2\ \text{M}$ ,  $[\text{CH}_2(\text{COOH})_2] = 0.06\text{--}1.2\ \text{M}$ , and  $[\text{HNO}_3] = 0.1\text{--}0.8\ \text{M}$ ), at different temperatures (Figures 3A and S7, Supporting Information). With the same flow of BZ reagents,  $\text{Gel}_a$ 's oscillating volume change decreases gradually when the temperature rises and is smallest at  $30\ ^\circ\text{C}$ .  $\text{Gel}_a$  exhibits its maximum volume change during oscillation with  $[\text{NaBrO}_3] = 0.2\ \text{M}$ ,  $[\text{CH}_2(\text{COOH})_2] = 0.4\ \text{M}$ , and  $[\text{HNO}_3] = 0.4\ \text{M}$ , at  $10\ ^\circ\text{C}$ , different from its optimal temperature for oscillation in static BZ solution,  $18\ ^\circ\text{C}$ .

To determine the optimal temperature for the other oscillating gels,  $\text{Gel}_b$  and  $\text{Gel}_c$  were tested under the same continuous flow at different temperatures. As shown in Figure 3B,  $\text{Gel}_b$  achieves its largest volume change at  $22\ ^\circ\text{C}$ . Both lowering and raising the temperature decrease the amplitude of oscillatory volume change dramatically. Like  $\text{Gel}_a$ ,  $\text{Gel}_b$  has a type I polymer network (Figure 2C), but the linker between the catalyst and the polymer backbone is shorter than in  $\text{Gel}_a$ .<sup>22</sup> In Figure 3C, the type II microgel,  $\text{Gel}_c$ , also has a maximal volume change at  $10\ ^\circ\text{C}$ . However, the volume change of  $\text{Gel}_c$  decreases more rapidly with temperature rising than does that of  $\text{Gel}_a$ . Moreover, there is almost no mechanical oscillation when the temperature is higher than  $22\ ^\circ\text{C}$ . Similar to our previous results on type II gels, high temperature produces a dense and rigid network of  $\text{Gel}_c$  that inhibits the oscillation. Because the ratio of monomers to additives in the polymer also affects the temperature response of the gels, it is expected that the three microgels would have different profiles of volume changes.

Comparing both types of gels' maximal volume change under continuous flow of BZ solution to their performance in static solution, continuous flow generally results in larger volume changes. As summarized in Figure 4A, under continuous flow, the average diameter change of  $\text{Gel}_a$  reaches 38% between the oxidized state and reduced state, which corresponds to a 163% volume change. In a bigger container filled with reaction solution without flow,  $\text{Gel}_a$  exhibits only a 4.6% volume change during oscillation. The continuous flow results in more than an

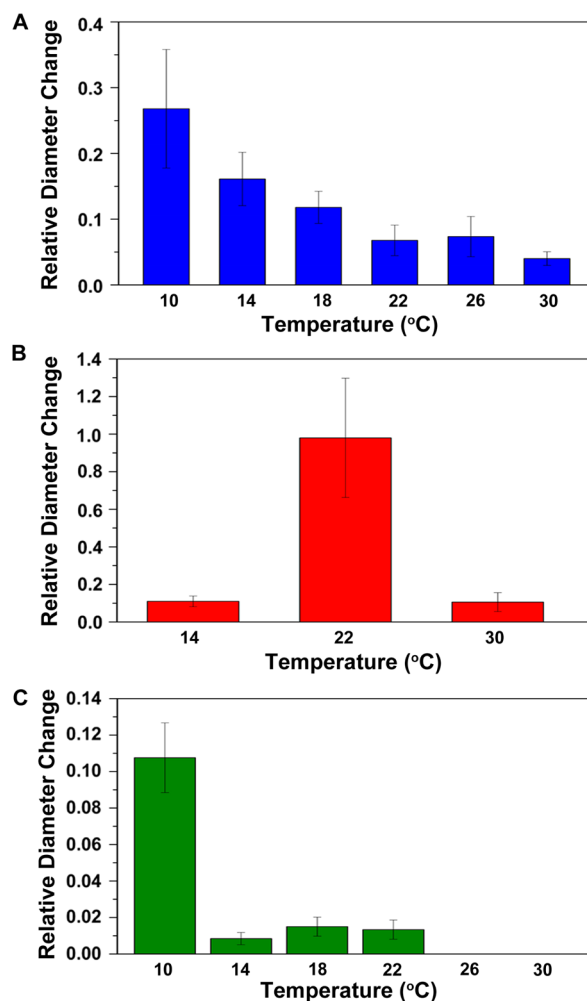


**Figure 3.** Relative volume changes of oscillating (A)  $\text{Gel}_a$ , (B)  $\text{Gel}_b$ , and (C)  $\text{Gel}_c$  under continuous flow of BZ solution ( $10\ \mu\text{L}/\text{min}$ ,  $[\text{NaBrO}_3] = 0.2\ \text{M}$ ,  $[\text{CH}_2(\text{COOH})_2] = 0.4\ \text{M}$ , and  $[\text{HNO}_3] = 0.4\ \text{M}$ ) at different temperature.

order of magnitude increase of the volume change. Under continuous flow, the average diameter change of  $\text{Gel}_b$  between its oxidized and reduced states reaches 100%, corresponding to more than a 500% volume change. Without the flow (i.e., in static BZ solution),  $\text{Gel}_b$  exhibits a 25% volume change (the best case). Unlike  $\text{Gel}_b$ ,  $\text{Gel}_c$  has a type II polymeric network (Figure 2C) and shrinks in the oxidized state.<sup>7</sup> Under continuous flow, the average diameter change of  $\text{Gel}_c$  is 16%, which corresponds to a 56% volume change. However, in stationary BZ solution,  $\text{Gel}_c$  only exhibits a 5% relative diameter change, which corresponds to a 16% volume change.

Besides inducing large oscillating volume changes, continuous flow slows the rate of oscillation of the gels. The oscillation periods of  $\text{Gel}_a$ ,  $\text{Gel}_b$ , and  $\text{Gel}_c$  are around 2000, 3600, and 1500 s under optimal continuous flow, but they are around 800, 250, and 400 s, respectively, under static conditions. These results further confirm that the flow decreases the rate of accumulation of the intermediates of the BZ reaction. By examining the correlation between oscillating volume change and oscillation period (Figure 5), we also found that larger volume change corresponds to a longer oscillation period and relatively larger standard deviation.

Considering the kinetic nature of the gel networks, it is not surprising that we observe batch differences and relatively large

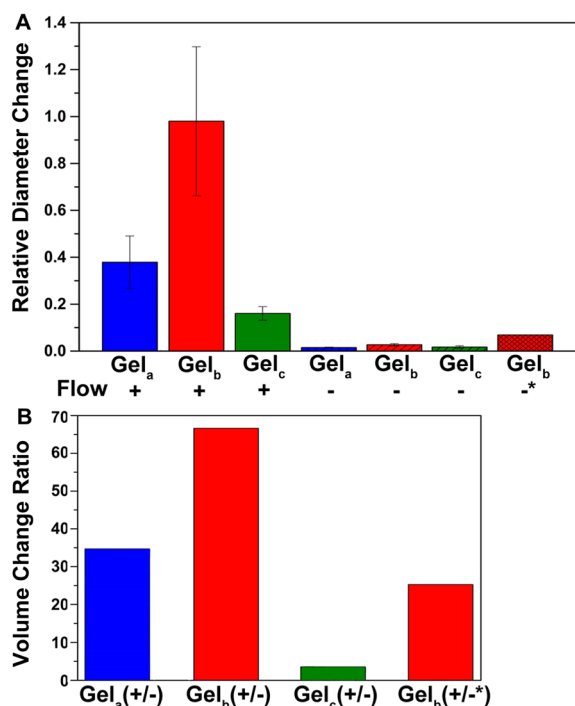


**Figure 4.** (A) Relative volume changes of oscillating gels at optimal rate of continuous flow and in static solution. (B) Volume change ratios for gels between optimal continuous flow and static solution (\*, largest volume change in previously reported static results<sup>19</sup>).

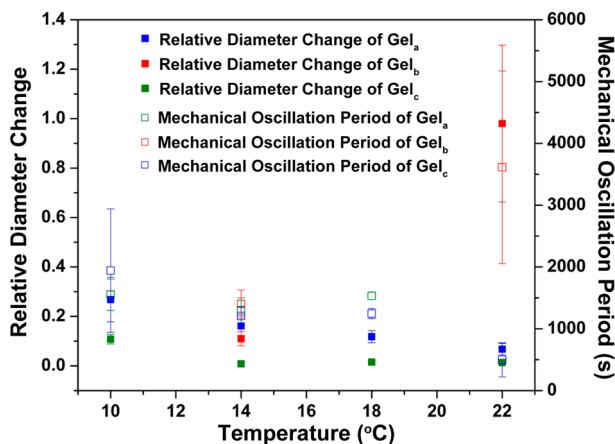


**Figure 5.** Temperature-dependent correlation between the oscillating volume change and mechanical oscillation period of Gel<sub>a</sub>, Gel<sub>b</sub>, and Gel<sub>c</sub>.

standard derivations. Since the larger volume change and longer oscillation period correlate with longer relaxation times, the gel networks also evolve with the chemical oscillation. This intriguing phenomenon becomes even more dramatic when the gel oscillates under continuous flow, further indicating the unique nature of spatially distributed chemical oscillation under flow.

By comparing the shapes and volumes of the microgels in the reduced state at the beginning of the BZ oscillation and after several hours of oscillation under continuous flow (Figure S10, Supporting Information), we found that the volumes of all three kinds of microgels increase considerably. This observation indicates that the networks of the microgels become less rigid during the BZ reaction due to the dynamic nature of the gels.

Because the microgels with larger oscillation volume change have longer oscillation periods, more extensive morphological changes occur in these gels. These morphological dynamics, resulting from larger changes of their polymer networks in the gel, thus contribute to the larger standard deviation.

The continuous flow also reveals that the geometry of the microfluidic channel influences the effect of flow rate on the volume change (Figure 6). As shown in Figure 6A, when the

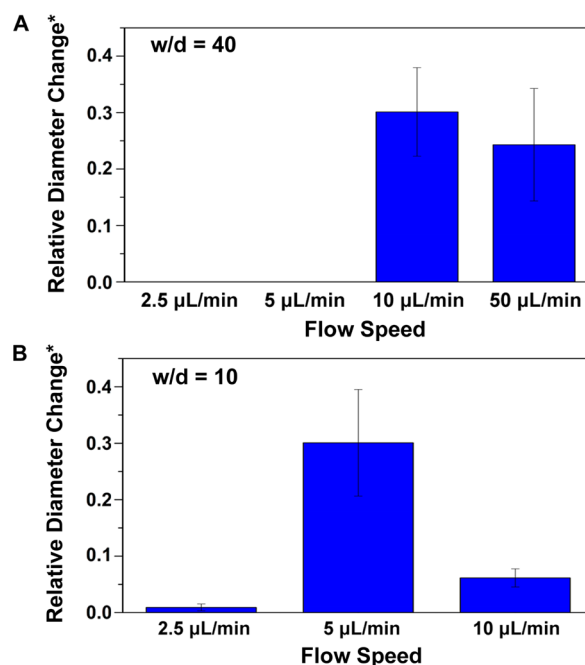


**Figure 6.** Relative diameter changes of Gel<sub>a</sub> in a microfluidic channel with  $w/d = 40$  (A) and a channel with  $w/d = 10$  (B) at different continuous flow speeds ( $w$ , width of microfluidic channel;  $d$ , diameter of microgel; \*, per oscillation).

width of the microfluidic channel is much larger than the diameter of the microgel (e.g.,  $w/d = 40$ ), Gel<sub>a</sub> shows no mechanical oscillations but only chemical oscillations at flow speeds of 2.5 and 5 μL/min. The biggest volume change of mechanical oscillation happens at a flow speed of 10 μL/min. Above 10 μL/min, changing the flow speed, even by a factor of 5, has little effect on the volume change of mechanical oscillation. However, when the width of the microfluidic channel is relatively smaller (e.g.,  $w/d = 10$ ), mechanical oscillation occurs at a flow speed of 2.5 μL/min, and the biggest volume change is achieved at 5 μL/min. Compared to  $w/d = 40$ , when  $w/d = 10$ , doubling the flow rate significantly affects the magnitude of the volume change (Figure 6B). Thus, higher flow speed is not only necessary but also ideal for mechanical oscillation when the width of the microfluidic channel is much larger than the diameter of the microgel. These experiments demonstrate that it is the fluid velocity in the channel that is important and not the flow rate.

Continuous flow contributes to two processes that have opposite effects on the oscillation of the gel. First, flow delivers the reagents needed in the reaction [ $\text{BrO}_3^-$ ,  $\text{CH}_2(\text{COOH})_2$ , and  $\text{HNO}_3$ ]. If the gel is operating in a diffusion-dominated regime, then increasing the flow rate will increase the concentration of reagents at the gel–solution interface, thereby increasing the rate of reaction. Eventually, the rates will become reaction-limited, and increasing the flow beyond this point will

not increase the chemical concentrations. However, flow also has an antagonistic effect on the oscillation through removal of essential products of the BZ reaction, such as  $\text{Br}_2$ , that are produced inside the gel and diffuse into the fluid stream and are subsequently swept away. Therefore, the reaction will cease when the flow rate is too high. With too little flow, the gel is starved, and with too much flow, essential chemicals produced by the gel are removed. Thus, it is reasonable that there is an intermediate flow rate for which there will be a maximal volume change.

The continuous flow provided by the microfluidic setup also allows quick and convenient screening or testing of other parameters of oscillating gels for chemomechanical conversion. For example, to probe the role of the counterion of  $[\text{Ru}(\text{bipy})_3]^{2+}$ , we flow acids with anions of different valence, in the sequences  $\text{HNO}_3\text{--H}_2\text{SO}_4$  and  $\text{H}_2\text{SO}_4\text{--HNO}_3$ . That is, after the microgel ( $\text{Gel}_1$ ) exhibits relatively stable oscillation in  $\text{HNO}_3$  (0.4 M), we change the  $\text{HNO}_3$  to  $\text{H}_2\text{SO}_4$  (0.2 M) in the flow stream of the BZ solution. Similarly, after the oscillation of the microgel becomes stable in  $\text{H}_2\text{SO}_4$  (0.2 M), we change the acid back to  $\text{HNO}_3$  (0.4 M). The relatively low concentrations of both acids ensure the constant acidity of the BZ solution. As shown in Figure 7A, replacement of nitric acid by sulfuric acid

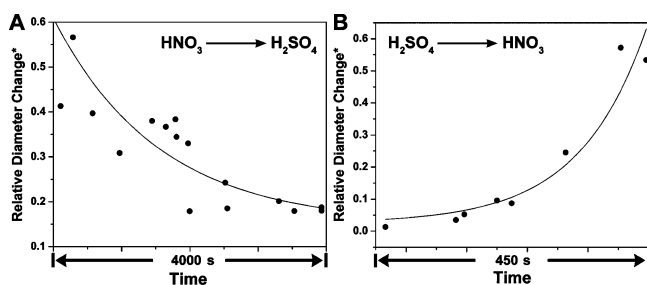


**Figure 7.** Chemomechanical oscillation profile during transition of  $\text{Gel}_1$  induced by counterion exchange (A) from nitric acid ( $\text{HNO}_3$ ) to sulfuric acid ( $\text{H}_2\text{SO}_4$ ) and (B) from  $\text{H}_2\text{SO}_4$  to  $\text{HNO}_3$ .

results in a decrease of the volume change (e.g., from 60% to 20% relative diameter change), accompanied by more rapid oscillation (e.g., the period decreases from 2000 to 1300 s, Figure S12A, Supporting Information). This process is reversible, though not symmetric, as switching sulfuric acid to nitric acid increases the volume change (e.g., from 5% to 60% relative diameter change, Figure 7B) and slows the oscillation (e.g., the period increases from 190 to 3500 s, Figure S12B, Supporting Information).

The smaller volume change caused by the use of sulfate probably arises from the buffering effect of the equilibrium between  $\text{HSO}_4^-$  and  $\text{SO}_4^{2-}$ , which makes the polymer network less sensitive to changes in the charge state of the catalyst (e.g., between  $[\text{Ru}(\text{bipy})_3]^{2+}$  and  $[\text{Ru}(\text{bipy})_3]^{3+}$ ).

Interestingly, it takes about 4000 s to stabilize the oscillation of the gel when nitric acid is replaced by sulfuric acid but only 450 s for the reverse transition from sulfuric acid to nitric acid. This result indicates that the in-gel ion exchange from  $\text{NO}_3^-$  to  $\text{SO}_4^{2-}$  is much slower than from  $\text{SO}_4^{2-}$  to  $\text{NO}_3^-$ , which is the first observation to date on the dynamic ion exchange that occurs in self-oscillating gels. These results confirm that the character of the electrolyte also impacts chemomechanical conversion in oscillating gels.

Coupled nonlinear chemical oscillators without flow have been studied as experimental models for understanding

biological phenomena,<sup>17,26</sup> ranging from the collective behavior exhibited by single cell organisms to neuronal circuits. Inspired by this, we combined microfabrication and microfluidics to make possible the study of the oscillatory behavior of an array of microgels under continuous flow. As shown in Figure 8A, we

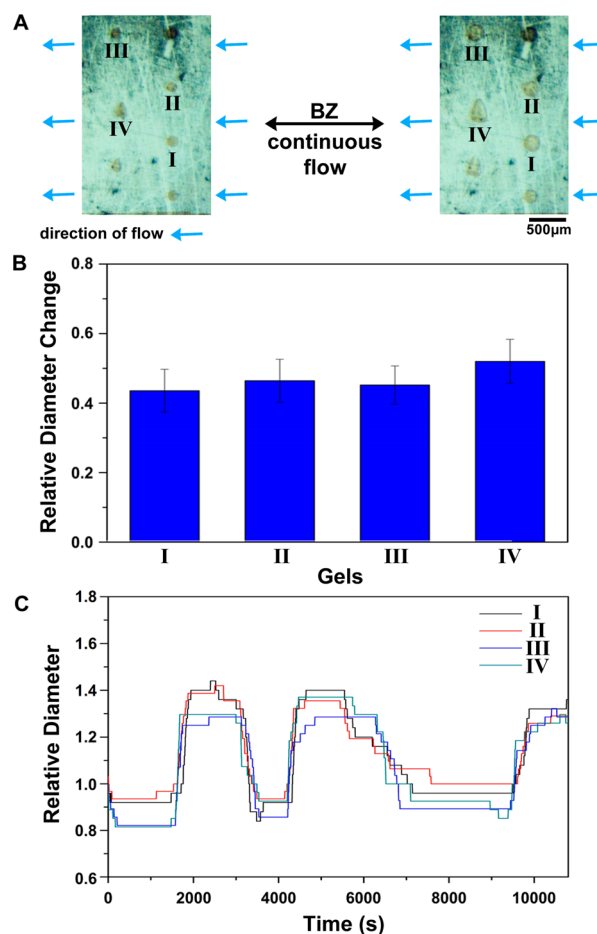


**Figure 8.** (A) Optical images of an array of  $\text{Gel}_1$  at different oscillation states under continuous flow ( $10 \mu\text{L}/\text{min}$ ). (B) Relative diameter changes of oscillating microgels at different positions in the array. (C) Oscillation profiles of the microgels (at positions I–IV) in the array.

made an array of microgels. By analyzing the oscillations of microgels at positions I–IV, we found that microgels at different positions in an array oscillated with similar relative volume change (Figure 8B). A plot of the time-dependent volume change (Figure 8C) of the microgels indicates that the microgels swell and deswell nearly simultaneously. The origin of coupling between oscillators without flow is diffusive flux of the participating components. It is known that the geometric arrangement, size, and shape of the oscillators and the distance between oscillators all affect the coupling strength and the resulting collective behaviors of the oscillators.<sup>27</sup> Applying a continuous flow of reagents to an oscillating microgel array significantly modifies the diffusive coupling of the participating species. Depending on the direction and speed of the flow, the coupling strength between oscillating microgels can be manipulated. As the first example of coupled oscillating microgel oscillators, this system provides a promising experimental model as a tunable coupling system that deserves further detailed study.

## CONCLUSION

This work, as the first example of using microfluidics to study chemomechanical transduction based on the BZ reaction, sets a new benchmark for the volume change of self-oscillating gels. Compared with classical thermal polymerization methods for the fabrication of BZ gels, photopolymerization has several advantages (e.g., speed, shape control, and size control), which should be useful for further exploration, such as the fabrication of hybrid oscillating gels consisting of different types of polymeric networks. The autonomous large volume change obtained in this work also differs fundamentally from the shape change of gels resulting from the alternating flow of different solutions (e.g., buffers with different pHs<sup>28</sup>). It is surprising that the parameters of the continuous flow corresponding to the microenvironment of the oscillating microgel affect so strongly their chemomechanical transduction.

Although it is known that the volume change can be related to the size of the BZ gel since traveling chemical waves give way to uniform oscillations in smaller systems,<sup>29</sup> the large difference in volume change observed in this case is unlikely to be caused by size differences in the microgels, since the microgels used have roughly the same size. The fact that the variation of the flow speed has a dramatic influence on the volume change suggests that the difference in volume change results primarily from the flow, which alters the reaction–diffusion profiles of the reactants, intermediates, and products of the BZ reaction.

The dependence of the volume changes of the gel on the rate of the flow of the BZ reagents implies that gradients of the reagents, intermediates, and products inside/outside of the BZ gels play an important role. Measurement of these gradients is a challenging experimental problem, which lies beyond the scope of the present work.

The combination of microfabrication and microfluidic techniques provides new and useful experimental tools for the development of theoretical frameworks for understanding chemomechanical materials based on a wide range of catalysts and polymeric networks.<sup>5,21</sup>

## ASSOCIATED CONTENT

### Supporting Information

Synthetic procedures, characterization methods, Figures S1–S12, and two videos showing the volume changes of Gel<sub>b</sub> and an array of Gel<sub>a</sub>. This material is available free of charge via the Internet at <http://pubs.acs.org>.

## AUTHOR INFORMATION

### Corresponding Author

[bxu@brandeis.edu](mailto:bxu@brandeis.edu); [epstein@brandeis.edu](mailto:epstein@brandeis.edu); [fraden@brandeis.edu](mailto:fraden@brandeis.edu)

### Author Contributions

<sup>§</sup>These authors contributed equally.

### Notes

The authors declare no competing financial interest.

## ACKNOWLEDGMENTS

This work was partially supported by grants from the Army Research Office (ARO 56735-MS), the National Science Foundation (CHE-1012428), the Pioneer Research Center Program of the National Research Foundation of Korea (2012-0001255), and by an NSF MRSEC grant (DMR-0820492). We thank Prof. Sukho Park for assisting the fabrication of the gels used in Figure 8.

## REFERENCES

- (1) Lodish, H.; Berk, A.; Kaiser, C. A.; Krieger, M.; Bretscher, A.; Ploegh, H.; Amon, A.; Scott, M. P. *Molecular Cellular Biology*, 7th ed.; W. H. Freeman: New York, 2012.
- (2) Duan, W.; Liu, R.; Sen, A. *J. Am. Chem. Soc.* **2013**, *135*, 1280. Sengupta, S.; Dey, K. K.; Muddana, H. S.; Tabouillot, T.; Ibele, M. E.; Butler, P. J.; Sen, A. *J. Am. Chem. Soc.* **2013**, *135*, 1406. Paxton, W. F.; Kistler, K. C.; Olmeda, C. C.; Sen, A.; St. Angelo, S. K.; Cao, Y.; Mallouk, T. E.; Lammert, P. E.; Crespi, V. H. *J. Am. Chem. Soc.* **2004**, *126*, 13424. Wang, Y.; Fei, S.-t.; Byun, Y.-M.; Lammert, P. E.; Crespi, V. H.; Sen, A.; Mallouk, T. E. *J. Am. Chem. Soc.* **2009**, *131*, 9926.
- (3) Osada, Y.; Okuzaki, H.; Hori, H. *Nature* **1992**, *355*, 242. Otero, T. F.; Sansinena, J. M. *Adv. Mater.* **1998**, *10*, 491. Yu, Y. L.; Ikeda, T. *Angew. Chem.-Int. Ed.* **2006**, *45*, 5416. Shinohara, S.; Seki, T.; Sakai, T.; Yoshida, R.; Takeoka, Y. *Angew. Chem.-Int. Ed.* **2008**, *47*, 9039. Zhao, Y. L.; Aprahamian, I.; Trabolsi, A.; Erina, N.; Stoddart, J. F. *J. Am. Chem. Soc.* **2008**, *130*, 6348. Liang, S. M.; Yu, Q. M.; Yin, H. Y.; Wu, Z. L.; Kurokawa, T.; Gong, J. P. *Chem. Commun.* **2009**, 7518. Zhou, Y. X.; Sharma, N.; Deshmukh, P.; Lakhman, R. K.; Jain, M.; Kasi, R. M. *J. Am. Chem. Soc.* **2012**, *134*, 1630. Dhanarajan, A. P.; Misra, G. P.; Siegel, R. A. *J. Phys. Chem. A* **2002**, *106*, 8835. Yoshida, R. *Adv. Mater.* **2010**, *22*, 3463. McDowell, J. J.; Zacharia, N. S.; Puzzo, D.; Manners, I.; Ozin, G. A. *J. Am. Chem. Soc.* **2010**, *132*, 3236. Zhang, Y.; Li, N.; Delgado, J.; Gao, Y.; Kuang, Y.; Fraden, S.; Epstein, I. R.; Xu, B. *Langmuir* **2012**, *28*, 3063. Suzuki, D.; Taniguchi, H.; Yoshida, R. *J. Am. Chem. Soc.* **2009**, *131*, 12058.
- (4) Yoshida, R.; Takahashi, T.; Yamaguchi, T.; Ichijo, H. *J. Am. Chem. Soc.* **1996**, *118*, 5134.
- (5) Dong, L.; Agarwal, A. K.; Beebe, D. J.; Jiang, H. R. *Nature* **2006**, *442*, 551.
- (6) Zhang, Y.; Li, N.; Delgado, J.; Zhou, N.; Yoshida, R.; Fraden, S.; Epstein, I. R.; Xu, B. *Soft Matter* **2012**, *8*, 7056. Yuan, P. X.; Kuksenok, O.; Gross, D. E.; Balazs, A. C.; Moore, J. S.; Nuzzo, R. G. *Soft Matter* **2013**, *9*, 1231.
- (7) Zhang, Y.; Zhou, N.; Akella, S.; Kuang, Y.; Kim, D.; Schwartz, A.; Bezpalko, M.; Foxman, B. M.; Fraden, S.; Epstein, I. R.; et al. *Angew. Chem., Int. Ed.* **2013**, *52*, 11494.
- (8) Field, R. J.; Noyes, R. M.; Koros, E. *J. Am. Chem. Soc.* **1972**, *94*, 8649. Epstein, I. R.; Vanag, V. K.; Balazs, A. C.; Kuksenok, O.; Dayal, P.; Bhattacharya, A. *Acc. Chem. Res.* **2012**, *45*, 2160. Bansagi, T.; Vanag, V. K.; Epstein, I. R. *Science* **2011**, *331*, 1309.
- (9) Beebe, D. J.; Moore, J. S.; Bauer, J. M.; Yu, Q.; Liu, R. H.; Devadoss, C.; Jo, B. H. *Nature* **2000**, *404*, 588.
- (10) Beebe, D. J.; Mensing, G. A.; Walker, G. M. *Annu. Rev. Biomed. Eng.* **2002**, *4*, 261. Wu, H. K.; Odum, T. W.; Chiu, D. T.; Whitesides, G. M. *J. Am. Chem. Soc.* **2003**, *125*, 554. Zheng, B.; Roach, L. S.; Ismagilov, R. F. *J. Am. Chem. Soc.* **2003**, *125*, 11170. Duffy, D. C.; McDonald, J. C.; Schueller, O. J. A.; Whitesides, G. M. *Anal. Chem.* **1998**, *70*, 4974.
- (11) Karns, K.; Vogan, J. M.; Qin, Q.; Hickey, S. F.; Wilson, S. C.; Hammond, M. C.; Herr, A. E. *J. Am. Chem. Soc.* **2013**, *135*, 3136. Puigmarti-Luis, J.; Rubio-Martinez, M.; Hartfelder, U.; Imaz, I.; Maspocho, D.; Dittrich, P. S. *J. Am. Chem. Soc.* **2011**, *133*, 4216. Price, G. M.; Chu, K. K.; Truslow, J. G.; Tang-Schomer, M. D.; Golden, A. P.; Mertz, J.; Tien, J. *J. Am. Chem. Soc.* **2008**, *130*, 6664.
- (12) Rossow, T.; Heyman, J. A.; Ehrlicher, A. J.; Langhoff, A.; Weitz, D. A.; Haag, R.; Seiffert, S. *J. Am. Chem. Soc.* **2012**, *134*, 4983.
- (13) He, M.; Novak, J.; Julian, B. A.; Herr, A. E. *J. Am. Chem. Soc.* **2011**, *133*, 19610. He, M.; Herr, A. E. *J. Am. Chem. Soc.* **2010**, *132*, 2512.
- (14) Zhang, H.; Tumarkin, E.; Peerani, R.; Nie, Z.; Sullan, R. M. A.; Walker, G. C.; Kumacheva, E. *J. Am. Chem. Soc.* **2006**, *128*, 12205.
- (15) Wu, H. K.; Huang, B.; Zare, R. N. *J. Am. Chem. Soc.* **2006**, *128*, 4194.
- (16) Runyon, M. K.; Johnson-Kerner, B. L.; Ismagilov, R. F. *Angew. Chem. Int. Ed.* **2004**, *43*, 1531.
- (17) Toiya, M.; Vanag, V. K.; Epstein, I. R. *Angew. Chem. Int. Ed.* **2008**, *47*, 7753. Delgado, J.; Li, N.; Leda, M.; Gonzalez-Ochoa, H. O.; Fraden, S.; Epstein, I. R. *Soft Matter* **2011**, *7*, 3155.

- (18) Ginn, B. T.; Steinbock, B.; Kahveci, M.; Steinbock, O. *J. Phys. Chem. A* **2004**, *108*, 1325.
- (19) Chen, I. C.; Kuksenok, O.; Yashin, V. V.; Moslin, R. M.; Balazs, A. C.; Van Vliet, K. J. *Soft Matter* **2011**, *7*, 3141.
- (20) Xia, Y. N.; Whitesides, G. M. *Angew. Chem. Int. Ed.* **1998**, *37*, 551.
- (21) Park, S.; Kim, D.; Ko, S. Y.; Park, J.; Akella, S.; Xu, B.; Zhang, Y.; Fraden, S. *Lab Chip* **2014**, *14*, 1551.
- (22) Chilkoti, A.; Dreher, M. R.; Meyer, D. E.; Raucher, D. *Adv. Drug Delivery Rev.* **2002**, *54*, 613. Sershen, S. R.; Westcott, S. L.; Halas, N. J.; West, J. L. *J. Biomed. Mater. Res.* **2000**, *51*, 293. Stile, R. A.; Burghardt, W. R.; Healy, K. E. *Macromolecules* **1999**, *32*, 7370.
- (23) Delgado, J.; Zhang, Y.; Xu, B.; Epstein, I. R. *J. Phys. Chem. A* **2011**, *115*, 2208.
- (24) Burstall, F. H. *J. Chem. Soc.* **1936**, 176.
- (25) Cho, S.; Ha, S. H. *Struct. Multidiscip. Optim.* **2009**, *38*, 53.
- (26) Vanag, V. K.; Epstein, I. R. *Phys. Rev. E* **2011**, *84*. Toiya, M.; Gonzalez-Ochoa, H. O.; Vanag, V. K.; Fraden, S.; Epstein, I. R. *J. Phys. Chem. Lett.* **2010**, *1*, 1241. Taylor, A. F.; Tinsley, M. R.; Wang, F.; Huang, Z. Y.; Showalter, K. *Science* **2009**, *323*, 614.
- (27) Tompkins, N.; Li, N.; Girabawe, C.; Heymann, M.; Ermentrout, G. B.; Epstein, I. R.; Fraden, S. *Proc. Natl. Acad. Sci. U. S. A.* **2013**, *111*, 4397.
- (28) Eddington, D. T.; Liu, R. H.; Moore, J. S.; Beebe, D. J. *Lab Chip* **2001**, *1*, 96.
- (29) Aihara, R.; Yoshikawa, K. *J. Phys. Chem. A* **2001**, *105*, 8445.